A PROBABILISTIC APPROACH TO SAWCUT TIMING AND DEPTH REQUIREMENTS FOR NEWLY CONSTRUCTED PORTLAND CEMENT CONCRETE PAVEMENTS

Jin-Hoon Jeong, Niraj Chapke, and Dan G. Zollinger, Ph.D., PE
Department of Civil Engineering, Texas A&M University
College Station, Texas 77843-3136, U.S.A.

This paper presents the details of an approach to account for the factors that have been found to affect the ability and probability of paving contractors to control cracking due to sawcutting in newly constructed concrete pavements. Variability in climate conditions and material characteristics during the hardening process affects the potential of cracking at any sawcut depth. Several factors such as material strength parameters, method and quality of curing, slab/subbase stiffness, and concrete shrinkage affect the probability of crack initiation. Others are relevant to concrete mixture characteristics that affect development of early aged stresses caused by shrinkage and thermally induced contraction.
This paper also presents the results of a probabilistic analysis of the factors that affect crack control using sawcut notches. A fundamental approach using a fracture mechanics is used to assure crack initiation in this paper.

INTRODUCTION

The control of cracking using sawcut notches in the surface of a concrete pavement is a complicated process involving several material, construction, and weather related factors. The successful control of cracking is further complicated by placement of the notch in appropriate time and depth combinations. The approach taken in this paper is to focus on the factors that have been found to affect the ability of paving contractors to control cracking in newly constructed concrete pavements during sawcutting operations. Many of these factors are relevant to concrete mixture characteristics that affect in one way or another development of early aged stresses caused by shrinkage and thermally induced contraction. These factors consist of:

1. Amount of water used in the concrete mixture
2. Amount of cement used in the concrete mixture
3. Method and quality of curing
4. Type of coarse aggregate used in the concrete mixture
5. Weather conditions at the time of construction
6. Time and depth of sawcutting
7. Type of slab base support and joint configuration
8. Slab thickness
9. Method of sawcutting/crack control

A variety of methods are available for crack control but discussion in this paper is limited to those based on the use of a concrete saw. Sawcutting methods are categorized as either conventional or early-entry. Conventional methods rely on the use of large, self-propelled saw

machines that consist of water-cooled saw blades. The saw blades on these machines rotate forward with respect to the direction of movement of the machines and cannot place a sawcut notch in the concrete surface until after sufficient hardening has occurred to prevent raveling and to ensure the durability of the joint. Although the type of coarse aggregate has an effect, most concrete mixtures must achieve a minimum of 3.45 MPa (500 psi) compressive strength to prevent unsightly raveling damage.

Early-entry saw machines are light-weight in comparison to water-based saws and do not require an external source of water to cool the blade. Early-entry saw blades rotate backward with respect to the direction of movement of the machines which make use of a patented skid-plate to prevent raveling. Typically, the notches placed with an early-entry saw can be placed as soon as one can walk on the concrete (which coincides with approximately one-half to two-thirds of the elapsed time between initial and final setting of the concrete). Concrete compressive strengths at this point are perhaps in the range of 0.17 to 0.34 MPa (25 to 50 psi).

Of the factors noted above, weather conditions at the time of construction may be the most important followed closely by the type of coarse aggregate. Both of these significantly affect sawcut timing and depth requirements. In conjunction with sawcut depth, the slab thickness affects the propensity of a notch to propagate a crack to the bottom of the slab.

The cracking analysis at a sawcut notch for a newly constructed jointed concrete pavement system provided in this paper systematically considered key factors at two different levels. The factors included within the scope of this format were limited within a restricted range of slab thickness and climatic factors as configured within a 2^3 factorial design that consists of 8 combinations of 1) Placement temperature, 2) Ambient relative humidity, and 3) Concrete aggregate type each at two different levels. The parameter levels are noted in Table 1. These combinations were considered for 3 different pavement thicknesses of 7.6, 15.2, and 22.9 cm (3, 6, and 9 inch) which included a special case of 8 additional combinations (relative to a 43.2 cm (17 inch) airfield pavement) where two levels of subbase friction were substituted for two levels of coarse aggregate type. The remaining factors not included in Table 1 were assigned constants that represent typical concrete mixtures, placing conditions, subgrade strengths, and curing methods for slab-on-grade construction.

Table 1 Factorial design of key sawcutting factors.

Level	Placement Temperature	Relative Humidity	Aggregate Type
Low	16 to 27°C	10 to 50%	Limestone
High	29 to 38°C	50 to 95%	River Gravel

The following discussion outlines the calculation process undertaken to conduct the cracking analysis. Prior to doing so, it is pointed out that when a pavement slab is placed in a thick ribbon of fresh concrete the temperature and moisture variations within the concrete are governed to a large extent by the climatic conditions at the time of placement (1, 2). It is while the concrete is in this state that other factors such as the quality of curing, the amount of cement, and the type of coarse aggregate used in the concrete have their greatest effects upon the cracking potential. Cracking in concrete pavements either occurs naturally or is induced at a mechanically placed notch. The forces behind the development of cracking are often due to temperature or shrinkage (due to moisture loss) differentials induced in the concrete while it is under going hardening.

Efforts to mechanically induce cracks at sawcuts notches are intended to take advantage of these differentials to force a crack at the notch location which introduces a discontinuity and a point of weakness in the concrete (which is why the crack initiates at the notch). Otherwise, uncontrolled cracks may occur in a somewhat random fashion at locations of maximum stress in the slab. This stress is caused by the temperature and shrinkage differentials (which is referred to as curling and warping stress) and is often large enough at some point in time to exceed the strength of the concrete. Whether cracks are induced or occur randomly, it is assumed that the stress in the concrete exceeds the strength of the concrete at the point of cracking.

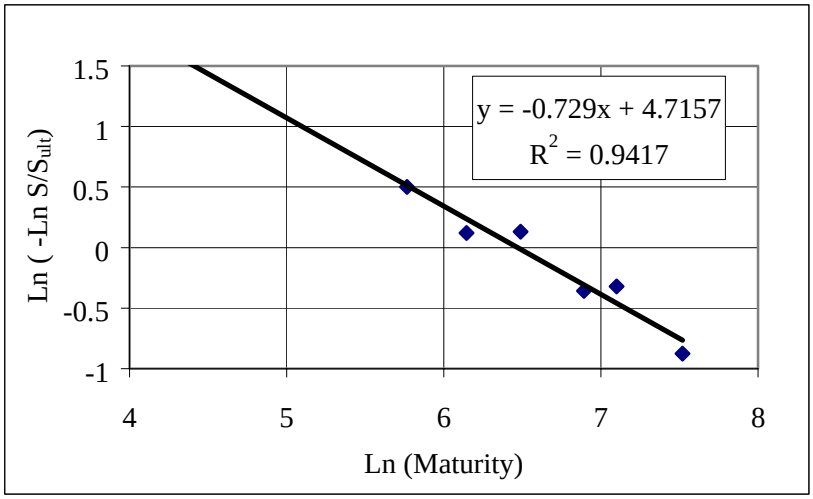

Figure 1 Assumed strength gain characteristics for a 5 sack concrete mixture (Note: y = Ln(-Ln α); x = Ln Maturity).

STRESS AND STRENGTH AT SAWCUT NOTCH

The process undertaken for this paper is to mathematically characterize the strength gain of the concrete for comparison to the stress development in the slab as a function of time. The characterization of the strength gain with time was done on a maturity basis where the relationship shown in Figure 1 was used to represent the gain in strength of a 5-sack concrete mixture during the curing and hardening process (3). Table 2 lists the ultimate split strength values used in the analysis. Young's modulus was based on the compressive strength of the concrete which was determined from the split tensile strength. Maturity is a parameter to represent the age of the concrete that correlates well with its strength over time. Concrete maturity is directly related to the temperature history of the concrete and consists of units of time and temperature. The temperature history of the concrete is affected by the heat of hydration and the ambient climatic conditions at the time of placement (4-6). In this paper, temperature modeling was conducted over a 30-hour period, which yielded the temperature patterns in the concrete as a function of time and location below the slab surface. And the temperature patterns allowed for the resultant maturity to be calculated. The temperature history was determined using the TMAC^2 software (7) as a function of the heat of hydration during the curing of the

Table 2 Ultimate split tensile concrete strength (MPa) (Note: split tensile strength = $7.5\sqrt{f_c'}$).

Coarse Aggregate Type	Low Temp. Cure	High Temp. Cure
Limestone	5.45	4.28
River Gravel	4.91	4.47

concrete. An example where temperature was predicted at various depths for one of the cases included in the factorial design above is shown in Figure 2.

The determination of stress was based on mathematical models representing the curling and warping behaviors of a concrete slab during the hardening process.

$$f_t = \frac{CE\varepsilon_{Tot}}{2(1-\nu)} \tag{1}$$

where

f_t = tensile stress,

C = stress coefficient $[=1-\frac{2\cos\lambda\cosh\lambda(\tan\lambda-\tanh\lambda)}{\sin 2\lambda\sinh 2\lambda}]$,

$\lambda = \frac{L}{\ell\sqrt{8}}$

L = free length or width of slab,

P = radius of relative stiffness,

E = elastic modulus,

ν = poisson's ratio of concrete (=0.15),

ε_{Tot} = unrestrained curling and warping strain $[= \alpha_t\Delta T_{eq} + \varepsilon_\infty\Delta(1\text{-}RH^3)_{eq}]$,

α_t = coefficient of thermal expansion of concrete, and

ε_∞ = ultimate shrinkage strain.

The ΔT_{eq} and $\Delta(1\text{-}RH^3)_{eq}$ terms are equivalent temperature and relative humidity difference between the pavement surface and bottom based on formulations given by Mohamed and Hansen (8). These equivalent differences are suggested to account for non-linear effects in either the temperature or humidity gradients on the curling and warping stress. In the case of temperature gradient, ΔT is defined at four locations below the pavement surface. The coordinate z is zero at mid depth of slab where upward is negative and downward is positive, and used in order to define coefficients B and D based on:

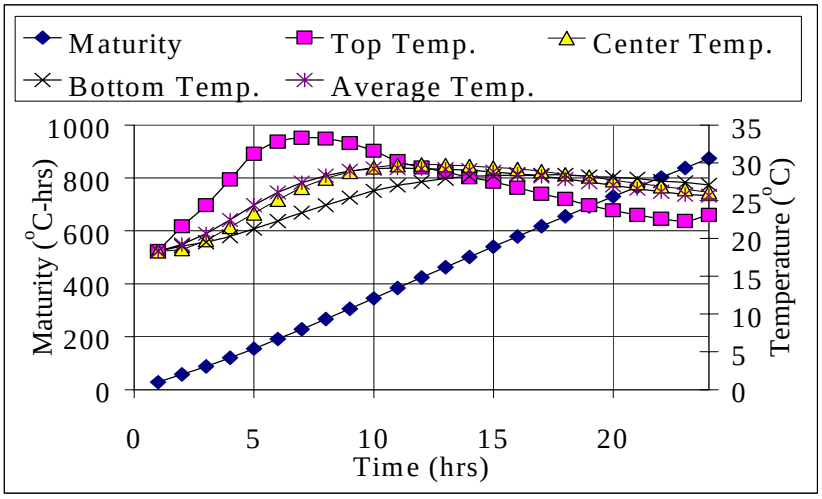

Figure 2 Maturity curve for a 22.9cm (9inch) placement under low temperature conditions.

$$\Delta T(z) = A + Bz + Cz^2 + Dz^3 \tag{2}$$

From these coefficients, ΔT_{eq} can be determined as:

$$\Delta T_{eq} = -12\left(\frac{Bh}{12} + \frac{Dh^3}{80}\right) \quad (3)$$

A similar approach can be applied to $\Delta(1\text{-}RH^3)_{eq}$. The results from Equation (1) are compared to those of Equation (4) to assess if cracking has occurred. The sensitivity of the concrete to crack initiation will depend upon the coarse aggregate type, concrete age, and the depth of the notch.

Key inputs into these models are the calculated temperature and the moisture shrinkage differentials that develop while the concrete curing is similar to those predicted in Figure 2. For this paper, these differentials were determined on an hourly basis for the first 30 hours after placement of the concrete pavement for each of the cases included in the factorial design. It is important to point out that many of the material properties included in the analysis are time dependent and consequently were adjusted from hour to hour. Figure 3 illustrates an example of the temperature differentials which occurred 11 hours after placement of the concrete. Figure 4 illustrates the pattern of stresses which result from the temperature and moisture differentials on an hourly basis for the first 30 hours after placement of the concrete. The zero hour represents the concrete age at placement which is coincidental with 8 a.m. in the morning. Also, shown in Figure 4 is the development of strength over the same time period. The strength of the concrete was correlated with maturity as previously noted, and when a notch was present in the slab, adjusted to account for its effect by the use of fracture mechanics.

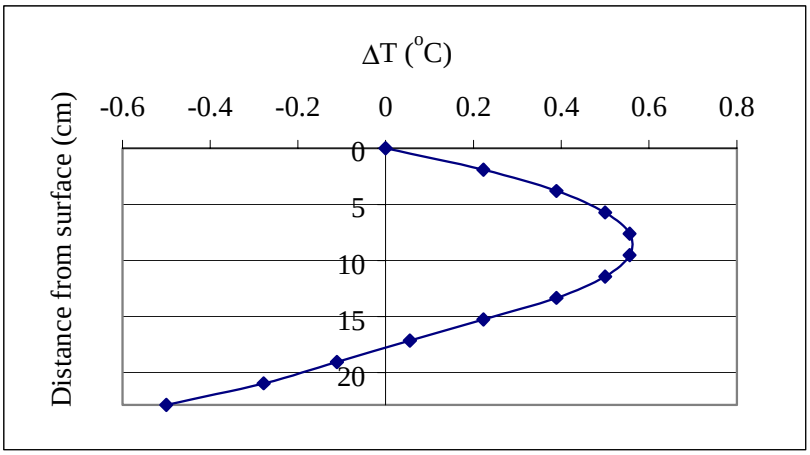

Figure 3 Temperature differentials in a hardening 22.9cm (9 inch) concrete slab after 11 hours of placement.

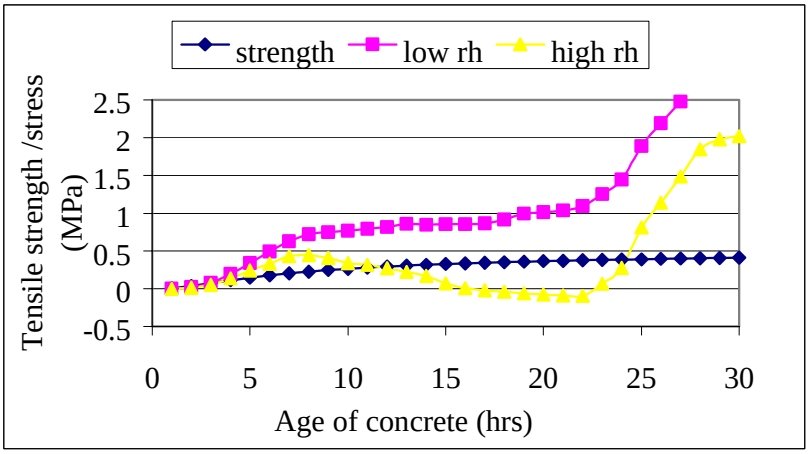

Figure 4 Stress and strength pattern at a sawcut notch depth to slab thickness ratio of 0.1 as a function of time under low temperature placement conditions.

Recent developments using fracture mechanics strength theories and a modified version of ASTM C 496 (9) have resulted in new approaches, specimen geometries, and strength

parameters that have allowed engineers to qualify the early-aged concrete strength relative to the bond between the aggregate and the paste. Use of fracture mechanics theories relates to crack development at an early age, which is inherently sensitive to coarse aggregate characteristics as they may relate to the aggregate-mortar bond. This sensitivity is referred to in terms of two fracture properties known as fracture toughness (K_{If}) and the length of the fracture process zone (c_f - a factor related to the brittleness of the concrete). Concrete brittleness is descriptive of a material's resistance to crack growth or the rate at which a crack may grow and, at an early age, is very sensitive to the type of coarse aggregate used in a concrete mixture. A test method based upon a modified split tensile specimens (Figure 5) based on ASTM C 496 determines K_{if} and c_f from 3 specimens of the same size (diameter).

Table 3 Concrete toughness parameters, K_{If} (MPa-$m^{1/2}$) and c_f (m).

Coarse Aggregate Type	Low Temp. Cure	High Temp. Cure
Limestone	0.99/0.69	0.90/0.61
River Gravel	0.77/0.53	0.69/0.48

$$f_t' = c_n \frac{K_{If}}{\sqrt{g'(\alpha_0)c_f + g(\alpha_0)d}} \quad (4)$$

where

f_t' = tensile strength of the concrete,
K_{1f} = fracture toughness ($FL^{-2}L^{1/2}$),
c_n = a constant based on specimen geometry (=1.0),
$\forall_0$ = initial crack ratio (=a_0/d),
d = slab thickness,
a_0 = sawcut depth,
$g(\forall) = \pi\alpha c_n^2 F^2(\alpha)$,
$g'(\forall) = \pi F^2(\alpha) + 2\pi\alpha c^2_n F(\alpha)F'(\alpha)$,
$F(\alpha) = 1.120 + 0.203\alpha - 1.197\alpha^2 + 1.930\alpha^3$, and
$F'(\alpha) = 0.203 - 2.394\alpha + 5.790\alpha^2$.

The function $g(\forall)$ and its derivative $g'(\forall)$ are dependent upon specimen geometry and evaluated where $\forall = \forall_0$. The two material factors, K_{If} and c_f, and the geometry functions evaluated at $\forall = \forall_0$ are used in Equation (4) to determine the nominal strength Φ_N of concrete corresponding to a particular fracture toughness. The nominal strength evaluated at a $\forall = 0$ will be equivalent to the split tensile strength of the concrete as determined by ASTM C 496. Both K_{If} and

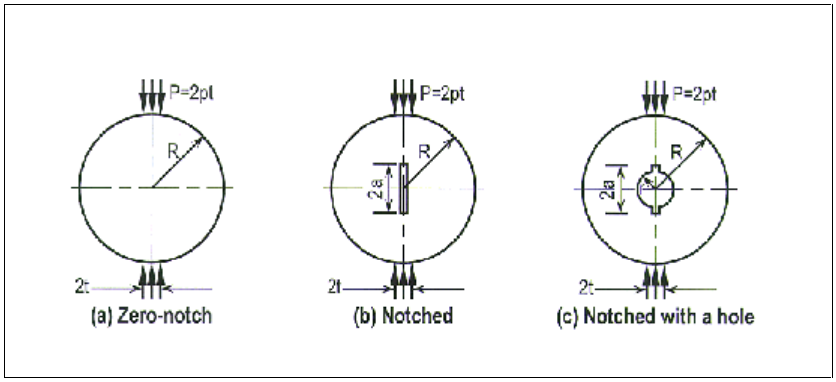

Figure 5 Split tensile test specimens for modified ASTM C 496 (9).

c_f are time dependent and consequently sensitive to aggregate bond strength at early concrete ages.

Table 4 Stress variance factors.

	Factor	COV (%)
Stress	Young's modulus	15
	Slab thickness	20
	k-value	20
	CTE	5
	Temperature difference	5
	RH difference	5
	Ultimate shrinkage	15
Strength	K_{If}	10
	C_f	10
	Sawcut depth to thickness ratio (α)	10

Several factors which contribute to the variability of strength and stress were also taken into account. The effects of factors on the variation above and below the mean of each of these parameters were assumed to be normally distributed. Based upon this distribution, the probability that the difference between the stress and the strength of the concrete at the tip of the sawcut notch is greater than zero was determined as a function of time from zero to 30 hours after placement of the concrete. In order to calculate this difference, both the variance of the distribution of stress and the strength of the concrete at the tip of the sawcut needed to be defined. The variances were developed from mean expression of stress and strength previously noted and the first order, second moment method:

$$Var\{Y\} = \sum_i \left[\frac{\partial Y}{\partial X_i}\right]^2 Var(X_i) + \sum_j \sum_{\substack{k \\ j \neq k}} \frac{\partial Y}{\partial X_j} Var(Y_j) \frac{\partial Y}{\partial X_k} Var(X_k)\rho \qquad (5)$$

where

Y = stress or strength,
X = variance factor (listed in Table 4), and
ρ = correlation factor.

For a given set of environmental conditions and slab thicknesses, an example of these probabilities and their associated trends with time for a given case is shown in Figure 6 along with the probabilities of a random crack occurring at the pavement surface over the same time interval. Figures A.1 in Appendix A represent differences in these probabilities at selected times (which is used to define the

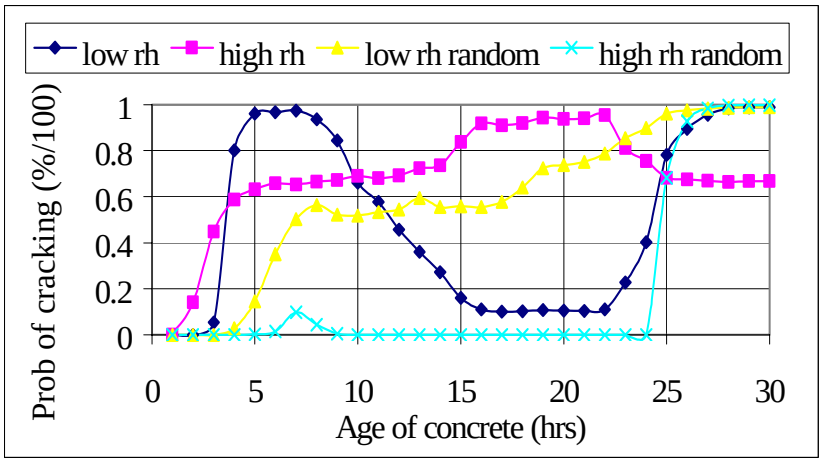

Figure 6 Stress and strength pattern at a sawcut notch depth to slab thickness ratio of 0.1 as a function of time under low temperature placement conditions.

probability of crack control). The advent of random cracking was based only on the amount of shrinkage in the concrete at the pavement surface due to the loss of moisture. The prediction of cracking at the sawcut notch was based on a combination of shrinkage and thermally-induced strains.

$$\sigma_{surface} = \left[\left(0.98 - RH^3\right)\varepsilon_\infty - \varepsilon_{crp}(t)\right]E(t) \quad (6)$$

where $\varepsilon_{crp}(t)$ is creep strain as a function of time (creep was varied from 25 to 100 microstrains over the 30 hour period).

The analysis of the probability of cracking for 15.2 cm (6 inch) and greater concrete thicknesses was based on a joint spacing of 4.6 m (15 feet) and a subgrade of average stiffness. The cracking charts for the 7.6 cm (3 inch) thickness were based upon the behavior of a thin-bonded overlay typical of what may be placed on a low-volume road consisting of an asphalt surface. Since these surfaces manifest greater stiffness than the average subgrade, an above average stiffness was used in the 7.6 cm (3 inch) thickness analysis. The analysis was also based upon the average cracking behavior of a concrete slab as it would occur under assumed trends in the temperature and humidity patterns within the designated limits previously noted. Given the premise that the scales of the climatic limits represent high and low extremes of the ranges in placement temperature and relative humidity, it can be reasonably assumed that, on the average, typical pavement cracking behavior will fall somewhere between the results associated with these extremes.

CRACKING PROBABILITIES

As previously noted, Table 1 itemizes the components of 8 combinations that are illustrated in an expanded form in Table 5. Each case shown in Table 5 was repeated each time for thickness 7.6, 15.2, and 22.9 cm (3, 6, and 9 inch). The analyses presented in this paper focuses on the control and incidence of transverse cracking as defined in terms of the difference between the probability of initiating a crack at the sawcut notch and the greatest probability of a random crack developing at or prior to the time of initiation. The differences associated with each of the cases shown in Table 5 are illustrated in bar charts provided in Appendix A with respect to:

Table 5 Climatic case combinations.

Case	Aggregate Type	Placing Temperature	Relative Humidity
1	Limestone	16 - 27°C	10 - 50%
2	River Gravel	16 - 27°C	10 - 50%
3	Limestone	29 - 38°C	10 - 50%
4	River Gravel	29 - 38°C	10 - 50%
5	Limestone	16 - 27°C	50 - 95%
6	River Gravel	16 - 27°C	50 - 95%
7	Limestone	29 - 38°C	50 - 95%
8	River Gravel	29 - 38°C	50 - 95%

1. Early-entry method of sawcutting,
2. Conventional method at the near-limit (the near limit occurs approximately 8 hours after placement of the concrete near the end of the day), and

3. Conventional method 24 hours after placement (when many sawcutting operations are undertaken).

Appendix A contains results for 7.6, 15.2, 22.9, and 43.2 cm (3, 6, 9, and 17 inch) thickness, where results for 43.2 cm (17 inch) are associated with airfield pavement construction. The 43.2 cm (17 inch) case considered only limestone aggregate but included subbase friction effects at high and low levels. This was done by adding a friction component to the stress analysis. In most instances, the differences are positive which means cracking can be controlled by sawcutting. But in cases where the differences are negative, cracking cannot be controlled by sawcutting. Each chart in Appendix A contains two results for the conventional method of sawcutting - one at the near limit and the other 24 hours after placement. The near limit is the earliest that a conventional or water-based saw can be feasibly used depending upon joint durability. The point of entry used for the early-entry method and the near-limit for the water-based saw is noted in Table 6. For this study, a moderate level of raveling was used as a basis for selecting the time associated with the near limit although, comparatively speaking, very little raveling damage typically results from use of the early-entry method.

Table 6 Time of sawcutting (hours after placement).

Coarse Aggregate Type	Method of Sawcutting	Low Temperature Placement	High Temperature placement
Limestone	Early entry	5	3
	Warter-based	8.5	7
River Gravel	Early entry	5	3
	Water based	9	8

Examination of each chart in the appendix clearly indicates the superiority of early-entry sawcutting over conventional methods with respect to the control of random cracking in jointed pavement construction. Prior to detailed discussions and as previously noted, the reader is again reminded that the results of each case shown in the appendix represent a bound in the range of cracking behavior that may occur under the climatic conditions delineated in Tables 1 and 5. The results in each of these bounding conditions are helpful in identifying limits associated with sawcutting operations. Typical cracking behavior can be derived from various combinations of the results at each climatic limit as to whether or not cracking can be controlled. In this respect, certain findings and conclusions can be drawn from each of the charts shown in the appendix. Upon examination of each chart, certain patterns in cracking behavior are repeated from chart to chart. These patterns are subsequently elaborated for the benefit of the reader based on discussion of the charts for the 22.9 cm (9 inch) slab which will lead to inferences regarding the results given in other charts. Due to the repeating nature of the cracking behavior, no further discussion of other charts is necessary except where cracking behavior deviates from those elucidated below.

As expected, the charts for the 22.9 cm (9 inch) slab using limestone or river gravel as coarse aggregate show greater potential for crack control under the early-entry system due to characteristically lower fracture toughness at an early age. This particular characteristic is also evident in the results shown in other charts. The chart of 22.9 cm (7.6 inch) slab using limestone aggregate for a paving mixture compares early-entry and conventional sawcutting at the near limit with respect to the probability of crack control in a slab. These results are shown at both a

high and low concrete temperature and a high and low relative humidity conditions at the time of paving. The use of the early-entry method shows similar results over this range of climatic conditions while the conventional method shows much lower potential particularly in the low temperature placement conditions. The lower potential in this instance is due to the notch depth extending too far below the effect of the stress gradient that is caused by the prevailing curing conditions. A similar set of circumstances exists for conventional sawcutting 24 hours after paving with the exception of the low humidity condition where cracking cannot be controlled. Similar conclusions and findings can be drawn from the comparisons made in the results shown in other charts in Appendix A. Exceptions to these trends are subsequently noted below.

It is interesting to note that the most stringent conditions for conventional sawcutting occurs with low temperature placements while the most stringent conditions for early-entry varies between high and low temperature conditions depending upon the slab thickness. It is also evident from the data shown in Appendix A that the thicker the pavement the easier it is to control cracking, particularly when the early-entry method is used (this observation is also in agreement with cracking behavior as predicted by fracture mechanic theories). Similarly with respect to the coarse aggregate type, cracking is easier to control in concrete using river gravel aggregate in comparison to limestone aggregate, as previously noted.

Table 7 Mix design and characteristics in 0.765 m^3 (1 cubic yard) of concrete.

Material	Proportions
Cement (type I)	221kg (488 lb)
Fly ash	56kg (123 lb)
Fine aggregate	508kg (1120 lb)
Coarse aggregate	840kg (1852 lb)
Water	123kg (271 lb)
Air entrainer	1.35%
Water/Cement ratio	0.44
Percentage of coarse aggregates	63%
Air content	2.4%
Slump	178mm (7.0 inch)
Concrete unit weight	2286kg/m^3 (142.73 lb/ft^3)

Referring to the results from the 22.9 cm (9 inch) slab, high temperature placements at low and high relative humidities using a limestone aggregate show greater probability to initiate cracking when conventional sawcut methods are used, but there is a greater probability of control of cracking when early-entry methods are used. In other words, the probability of initiation may be greater in some cases for deeper sawcuts, a greater risk of random cracking generally accompanies these probabilities. Other similar results can be found in the 15.2 cm (6 inch) cases for high relative humidity placements using both limestone (at both low and high temperature) and river gravel aggregates (at low temperature only); high temperature, low relative humidity conditions for 7.6 cm (3 inch) placements using both limestone and river gravel aggregates. The 7.6 cm (3 inch) early-entry placements were determined at a sawcut depth of 1.3 cm (one-half inch). Results for the 43.2 cm (17 inch) cases indicate early-entry method is the only feasible method to control cracking on high friction subbases although the chances of control are slim in low relative humidity conditions.

FIELD SLAB AND SAWCUT INSTRUMENTATION

To verify the concept of probabilistic approach in cracking control suggested in this paper, a field concrete slab was made and a combination of cases shown in Table 5 is given. The placement of a concrete slab was done at the Riverside Campus Annex test facility of the Texas A&M University at College Station, Texas. Before the slab, a 10.2 cm (4 inch) thick lean subbase was placed. The subbase was 10.4 m (34 ft) long and 4.3 m (14 ft) wide. The construction consisted of a 30.5 cm (12 inch) slab 9.2m (30 ft) long and 3.7 m (12 ft) wide. The concrete mix design consisted of 6 sacks of Type I cement per 0.675 m^3 (cubic yard) with 20% of fly ash. The coarse aggregates were crushed limestone and the fine aggregates were natural sand. Field test indicated a water-cement ratio of 0.44, a 10.2 cm (4 inch) slump and 2.4 % of an air content. Table 7 shows the concrete mixture proportions. The slab was instrumented for moisture, temperature, strain, and displacement to provide data with which to verify the theoretical expressions used to predict crack initiation.

CRACKING CONTROL IN TEST SLAB

A transverse sawcut joint was made at a concrete age of approximately 3 hours, as noted in Table 6, at the longitudinal center of the slab placement. Drying shrinkage, a main cause of cracking, has both reversible and irreversible components. However, with time and drying and re-wetting cycles, the process becomes mostly reversible (4, 5). Usually the irreversible part of shrinkage represents between 30 and 60 % of the total drying shrinkage. The fully reversible shrinkage is due to additional links within the C-S-H gel during drying, when closer contact between the gel particles occurs. If the cement paste has hydrated to a high degree before drying, it will be less affected by their contact. Reversible shrinkage is related to capillary stress, disjoining pressure, and change in surface free energy within the C-S-H gel. Irreversible shrinkage is mostly dependent on porosity and increases as drying increases. The factors which affect irreversible shrinkage are pore size, bonding in C-S-H, and pore water distribution. Different kinds of shrinkage occur in concrete due to evaporation. Plastic shrinkage may also contribute to cracking particularly when the evaporation is greater than the bleeding rate. As will be discussed, the bleed channels maybe contribute to cracking by causing a point of weakness in the matrix of the hardening concrete. The bleed channels, in effect, are small flaws. These flaws lead to stress concentrations in a very small volume under shrinkage strain ultimately causing the strength to be exceeded in the material with a consequent of microscopic fracture (9, 10). Since concrete is a notch sensitive material, a notch in the surface of a concrete pavement can initiate a

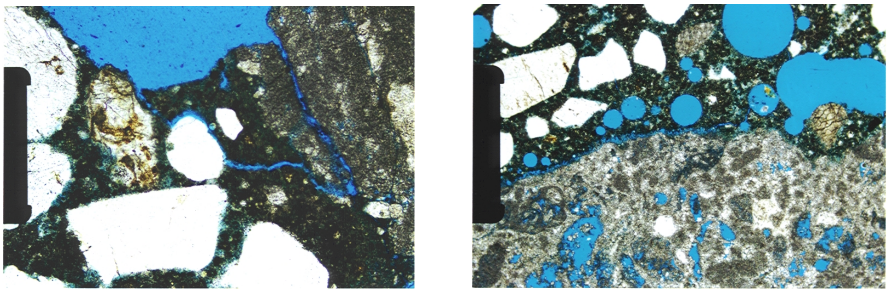

(a) At notch tip. (b) At aggregate perimeter.

Figure 7 Cracks follow capillary channels.

crack. As a result, crack propagates from the bottom of the notch to the bottom of the slab. As this occurs, other stresses in the slab due to environmental effects are reduced. Figure 7 (a) is a close up of notch tip and cracks are propagating from the notch tip because of the stress concentration. Greater porosity at the aggregate perimeters than in cement paste as shown in Figure 7 (b). This greater porosity coincides with the matrix bleed channels and is consequently a source of cracking in early aged concrete.

Thermal strain and shrinkage develop due to temperature and relative humidity differences mentioned above. The sum of the strains is called total strain difference and can be calculated as shown in Equation (1). Immediately after the placement of the concrete slab, temperature at top of the slab is greater than that at bottom, and relative humidity at top is smaller than that at the bottom. So both temperature and relative humidity affect the expansion of the slab at any time. Initially, a compressive strain resulted at the top and a tensile strain at the bottom near joint. But later, a temperature at top is smaller than that at bottom and relative humidity at top is greater than that at bottom. A tensile strain resulted at the top and a compressive strain at the bottom about 8 hours after placement of slab, as shown in Figure 8.

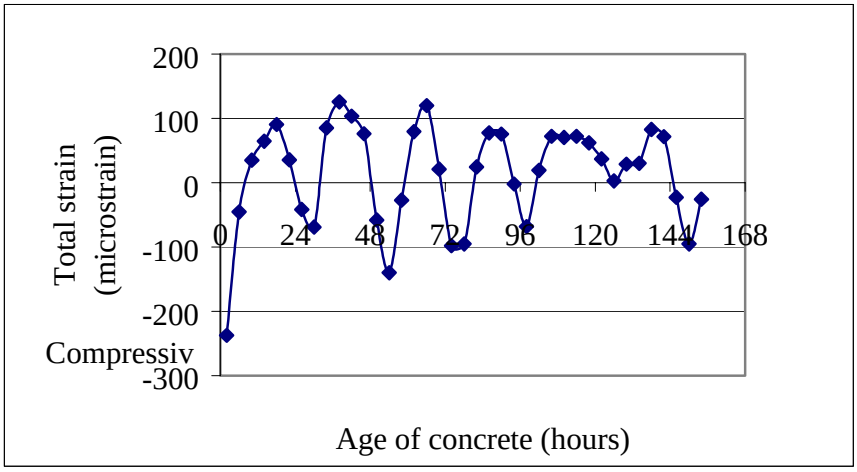

Figure 8 Total strain environmentally developed at top surface.

To identify the tensile and fracture strength development of the slab concrete, strength tests were conducted at 3rd, 7th, and 14thday. The fracture parameters (K_{If} and c_f) determining the tensile strength with time were found from the tests and the results are shown in Table 8. Using the fracture parameters, tensile strength at each point of time can be calculated by Equation (4).

Table 8 Fracture parameters and tensile strength estimated.

Time (day-hour)	K_{If} (MPa-$m^{½}$)	C_f (mm)	f_t' (MPa)
3-77	0.043	0.24	0.51
7-171	0.036	0.16	0.43
14-338	0.057	0.42	0.66

From the estimated tensile strength development model, initial 24 hours tensile strengths can be predicted and they are compared to the tensile stress occurring at the bottom of the sawcut. When tensile stress at the bottom of the sawcut is larger than the tensile strength, a crack propagates from the bottom of the sawcut to bottom of the slab. To predict the tensile stress at each point of time, elastic modulus and total strain composed of thermal strain and shrinkage must be calculated. Elastic modulus

develops as hydration of concrete progresses and compressive strength develops. The degree of hydration and maturity can be correlated as (11):

$$\ln \alpha = -\left(\frac{b}{M}\right)^{a} \tag{7}$$

where

α = degree of hydration,
M = maturity, and
a, b = variables correlating degree of hydration and maturity.

The variables, a(=1.492) and b(=545), can be determined from degree of hydration and maturity data found from compressive strength test and maturity data acquired at 0.5th, 3rd, 7th, and 14th days. The tensile stress at the bottom of sawcut at each point of time is calculated on the based of Equation (1). The tensile stress at bottom of sawcut became larger than tensile strength about 11 hours after placement of slab as shown in Figure 9. Observations from the test site indicated that cracking initiated approximately 11 to 12 hours after placement. The combination of the cases in this field slab is limestone aggregate, high temperature, comparatively low relative humidity, and early-entry. Referring to Figures A.1, high probability of control is expected in this combination of case and this expectation agrees with the mechanical calculations and observations well.

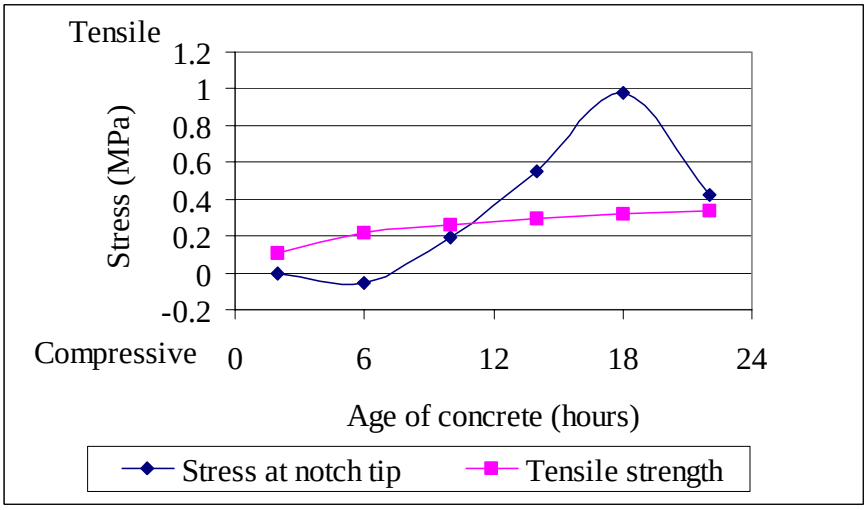

Figure 9 Possibility of crack occurrence at bottom of sawcut.

CONCLUSIONS

Variable climate conditions and material characteristics were used as factors in a probabilistic approach for cracking control due to sawcutting to find the most desirable sawcut depth and timing.

Greater potential for crack control exists under the early-entry system due to characteristically lower fracture toughness of the concrete in the slab for both limestone aggregate and river gravel aggregate cases. The most stringent conditions for conventional sawcutting occurs with low temperature or relative humidity placements while the most stringent conditions for early-entry varies between high and low temperature / relative humidity conditions depending upon the slab thickness and the magnitude of the temperature or shrinkage gradient. It is also evident that the

thicker the pavement the easier it is to control cracking, particularly when the early-entry method is used. With respect to coarse aggregate type, cracking is easier to control in concrete using river gravel aggregate in comparison to limestone aggregate. From the results, it can be said that the probability of initiation may be greater in some cases for deeper sawcuts but a greater risk of random cracking generally accompanies these probabilities.

From both an operational and cost standpoint, it is evident for the environmental conditions considered that early-entry sawcut methodology holds a significant advantage over conventional methods as defined in this paper. In many of the cases considered, early-entry sawcut notches maintained greater potential to initiate and control cracking than notches placed at later concrete ages and at greater depths. On the average, this translates into lower risks, lower costs, and greater profit margins when early-entry sawcut methods are used in the construction of jointed concrete pavements.

REFERENCES

1. Byfers, J. *Plain Concrete at Early Ages.* Research 3:80, Swedish Cement and Concrete Research Institute, Stockholm, Sweden, 1980.
2. Bruegel, K.V. *Simulation of Hydration and Formulation of Structure in Hardening Cement-Based Materials.* Doctoral Thesis, Delft University of Technology, Netherlands, 1991.
3. Malhotra, V.M. *Maturity Concept and the Estimation of Concrete Strngth.* Information Circular IC 277, Department of Energy Mines Resources (Canada), Mines Branch, No. 1971.
4. Neville, A.M. *Properties of Concrete.* 4th edition, John Wiley & Sons, Inc., 1996.
5. Mindess, S. and Young, T.F. *Concrete.* Prentice-Hall Inc., Englewood Cliffs, New Jersey, 1981.
6. Yang, S.C. *A Temperature Prediction Model in New Concrete Pavement and A New Method for Concrete Fracture Parameters.* Ph.D. Dissertation, Texas A&M University, College Station, 1996.
7. Wang, L. *Early Age Characterization of Concrete Temperature and Moisture Parameters.* Ph.D. Dissertation, Texas A&M University, 2001.
8. Mohamed, A.R. and Hansen, W. *Effect of Nonlinear Temperature Gradient on Curling stress in Concrete Pavement.* Transportation Research Record 1568, Transportation Research Board, Washington D.C., 1996, pp. 65 - 71.
9. Tang, T., Yang, S.C., and Zollinger, D.G. *Determination of Fracture Energy and Process Zone Length using Variable-Notch One-Size Specimens.* ACI Materials Journal, Vol. 96, No. 1, Jan.-Feb. 1999, pp. 3-10.
10. Griffith, A.A. *The Phenomena of Rupture and Flow in Solids.* Philosophical Transactions, Series A, 221, Royal Society, 1920.
11. Malhotra, V.M., Carino, N.J. *CRC Handbook on Nondestructive Testing of Concrete.* CRC Press, 1991.

APPENDIX A

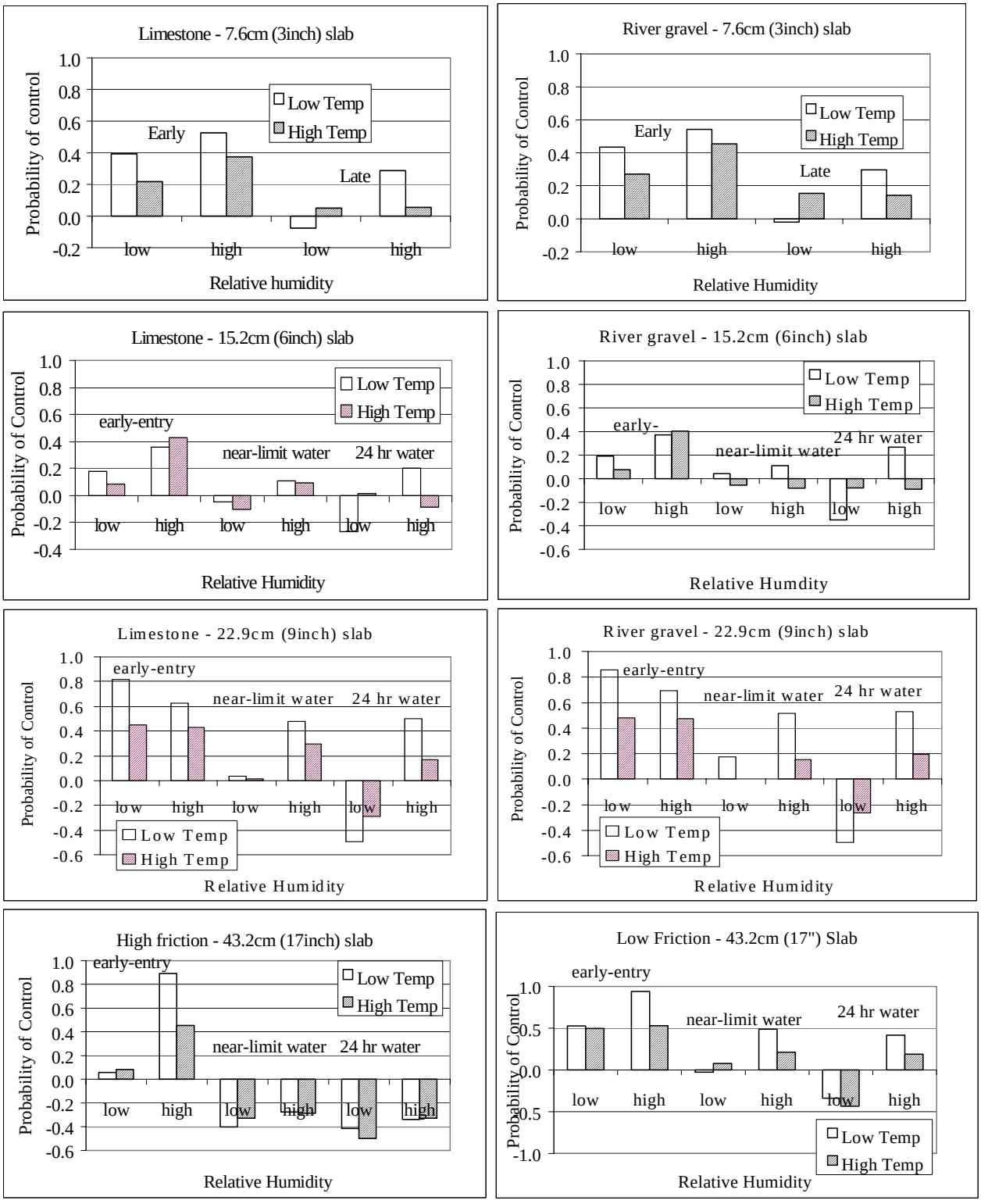

Figures A.1 Differences in the Probability of a Crack occurring at a Sawcut Notch versus at a Random Location.